Analysis of the fluidization behaviour and application of a novel spouted bed apparatus for spray granulation and coating

O. Gryczka[1], S. Heinrich[1], M. Jacob[2], N.G. Deen[3] and J.A.M. Kuipers[3]

[1] Institute of Solids Process Engineering and Particle Technology, Hamburg University of Technology, Denickestr. 15, 21073 Hamburg, Germany
[2] Glatt Ingenieurtechnik GmbH Weimar, Nordstraße 12, 99427 Weimar, Germany
[3] Faculty of Science and Technology, University of Twente, PO Box 217, 7500 AE, Enschede, The Netherlands

Abstract

Spouted beds are well known for their good mixing of the solid phase and for their intensive heat and mass transfers between the fluid phase and the solid phase. Nearly isothermal conditions are enabled which is of advantage for the treatment of granular solid materials in granulation, agglomeration or coating processes. In this work the hydrodynamic behaviour of a novel spouted bed apparatus with two horizontal and slit-shaped gas inlets is investigated by high-frequency recordings of the gas phase pressure fluctuations over the entire bed. The hydrodynamic stable operation domain, which is of importance for operating the apparatus, will be identified and depicted in the Re-G-Ar-diagram by Mitev [1]. Another focus of this work is the simulation of the spouting process by application of a continuum approach in FLUENT 6.2. The effect of the frictional stresses on the hydrodynamic behaviour is examined by performing simulations with and without consideration of friction. The angle of internal friction ϕ_i in Schaeffer`s [10] model will be varied and the simulation results will be compared with experiments. It was found that the influence of friction is not very big by application of the quite simple and empirical frictional viscosity model by Schaeffer [10] basing on soil mechanical principles. Also the simulation results under negligence of friction were similar to those under consideration of friction. Another part of this work is the industrial application of the novel spouted bed in granulation and coating processes. Compared to classical fluidized beds, a much narrower particle size distribution, a higher yield and a higher product quality was obtained in the novel spouted bed.

Keywords: Spouted Bed, CFD modelling, Granulation, Coating, Granular flow

1. Introduction

Recently the importance of the spouted bed technology has significantly increased in the context of drying processes as well as granulation, agglomeration or coating. The main difference of spouted beds in comparison with conventional fluidized beds is the variable cross section area of the apparatus as function of the apparatus height. Contrary to fluidized beds where particle motion happens randomly, the particles in spouted beds perform a continuous circulating motion. Thus, more defined heat- and mass transfers provide excellent conditions for the injection of liquids yielding a higher product quantity and quality in industrial applications. The knowledge of the stable hydrodynamic operation range of the spouted bed, which is smaller compared to conventional fluidized beds, is of importance for operating the apparatus. The first part of this work deals with the experimental investigation of the hydrodynamic behaviour of a novel prismatic spouted bed apparatus with two horizontal and slit-shaped gas inlets. By measured gas phase pressure fluctuations and Fourier analysis on these spectra, the hydrodynamic stable operation range will be identified and depicted in the dimensionless Re-G-Ar-diagram by Mitev [1]. The particle system, the gas throughput and the cross section area of the gas inlets (by rotation of the cylinders for gas

flow regulation) will be varied. With the results of this work, a comparison will be made with stable operating ranges of other fluidized beds and spouted bed apparatuses, which already have been characterized by several authors (Kojouharov [2]; Mitev [1]; Piskova [3],[4]).
Modelling of spouted beds by means of modern simulation tools, like discrete particle models or continuum models, has become a precious opportunity to understand the complexity of multiphase flows in these apparatuses. In this work, two-dimensional continuum simulations of this novel kind of spouted bed with adjustable gas inlets are presented. Recently Gryczka et al. [5], [6], [**7**] performed CFD continuum simulations in this spouted bed testing different gas-particle drag models and studied the influence of the coefficient of restitution on the hydrodynamic behaviour. They found a qualitative good agreement of the simulation results with experiments by application of the Clift et al. [8] drag model, whereas the bed expansion was slightly under-predicted. Different values of the coefficient of restitution which describes the energy dissipation due to non-ideal particle collisions lead to a modified hydrodynamic behaviour. The best fit with experimental findings was obtained with a value of 0.75 which constitutes a realistic value for the experimental material (monodisperse and spherical γ-Al_2O_3 particles) as reported by Antonyuk et al. [9]. In this work, the influence of the frictional contribution on the hydrodynamic behaviour will be investigated. Simulations with and without consideration of frictional stresses will be carried out. Moreover a numerical study under variation of the angle of internal friction in Schaeffer`s [10] model will be presented. Huilin et al. [11] revealed in their investigations of a 2-D conical spouted bed by application of a continuum model that the shape of the spout, the annulus and the fountain changed appreciably when the frictional stresses were changed, demonstrating the significant effect of the frictional stress on the dense particle flow especially in the annulus. In the end of this work industrial applications are presented. Based on the novel spouted bed apparatus the German company *Glatt* has developed the innovative ProCell - processing unit for processes like granulation, agglomeration or coating.

2. Experimental

For experimental investigations to describe the hydrodynamic behaviour, a prismatic spouted bed apparatus was constructed, which consists of transparent acryl-glass with two horizontal and adjustable gas inlets. Figure 1 shows a photo and a flow chart of the spouted bed apparatus.

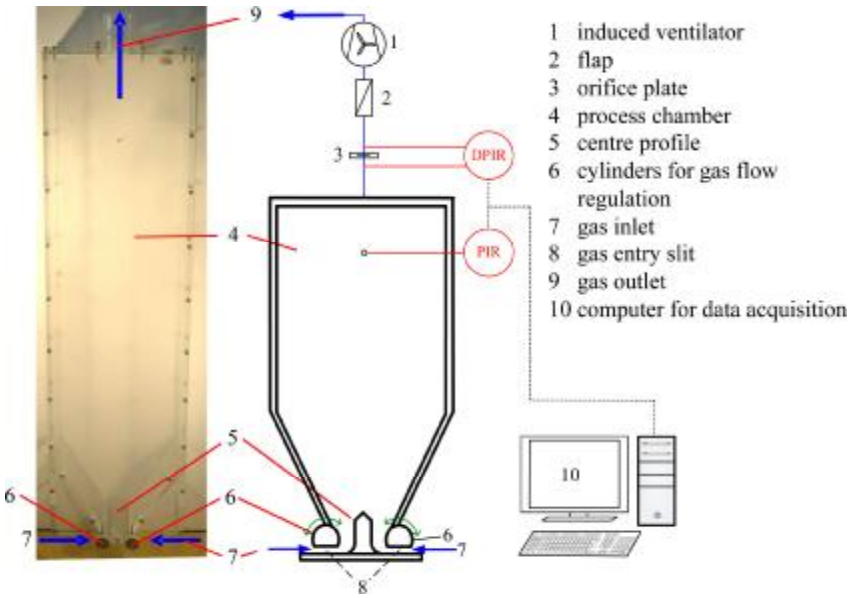

Figure 1 Photo and flow chart of the investigated acryl-glass spouted bed apparatus.

Determination of the stable spouting range of the investigated spouted bed apparatus

In the following, an example of the determination of the stable operation range by visual observations and by analysis of measured gas phase pressure fluctuations by the fast Fourier transformation algorithm (FFT) will be demonstrated. The bed material consists of γ-Al_2O_3-particles (d_s = 1.75 mm, ρ_s=1040 kg/m^3, sphericity Θ=0.98) and the bed mass was 1.0 kg. At each set of parameters (particle system, angle of the cylinders for gas flow regulation, bed mass and gas throughput) 10.000 values of the overpressure were measured during a period of 10 seconds and subsequently the FFT was applied to these values. Figure 2 shows the bed pressure drop with indication of the points of different gas volume flows where the results of the Fourier analysis will be presented.

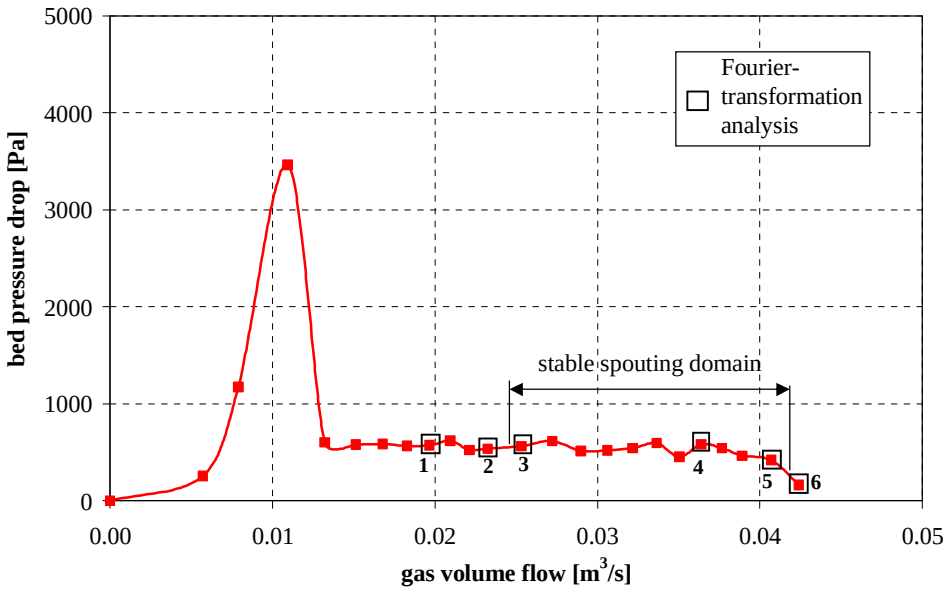

Figure 2 Measured bed pressure drop and indication of the points for the fast Fourier algorithm.

In Figure 3 the results of the measurement of the gas phase pressure fluctuations and of the FFT for the points 1 to 6 are presented and conclusions on the hydrodynamic behaviour can be made. The amplitudes of the gas fluctuations indicate the existence of pressure impulses which originate from bursting gas bubbles on the bed surface. From Figure 3a it can be extracted that about 4 to 5 main fluctuations per second were detected at a gas volume flow of 0.020 m^3/s that are not fairly equal and exhibit different amplitudes. Also the FFT indicates that there is a commanding frequency of about 5 Hz, but there are further frequencies between 2 and 4.5 Hz as well as between 5.5 and 7 Hz which cannot be neglected. That means that rising gas bubbles of different sizes burst on the bed surface at irregular time intervals. From visual observations one can see that bed expansion is very low and that big and small bubbles move upwards through the bed causing more or less powerful pressure impulses. Also the total bed movement is more similar to a fixed bed state, i.e. the particle mixing caused by the fluidization gas, is very low. This operation range is referred to as the "bubbling" state and is instable by definition as reported earlier by Piskova [3], [4].

By increasing the inlet gas volume flow, this instable spouting state remains unchanged (see Figure 3b). When the gas throughput is increased to 0.025 m^3/s (Figure 3c) a change can be recognized compared to the previous graphs. Now, the main fluctuations are equal and have nearly the same amplitudes which results in a large dominant peak in the FFT. The position of this peak on the x-axis reflects the frequency of the main fluctuation. This spouting operation is called stable. Hence, the turnover between the bubbling instable and the stable operation lies between the gas volume flows of 0.023 m^3/s (Figure 3b) and 0.025 m^3/s (Figure 3c). The stable spouting range is characterized by a circulating particle motion and a good particle mixing without dead zones. With

enhancement of the gas flow (see Figure 3d and e) the spouting process remains stable. At a gas volume flow of 0.042 m^3/s (Figure 3f), the main fluctuations are not uniform anymore and exhibit different amplitudes. The upper boundary of the stable operation range is reached and the process is thus instable. The range of stable spouting for this parameter set is depicted in Figure 2.

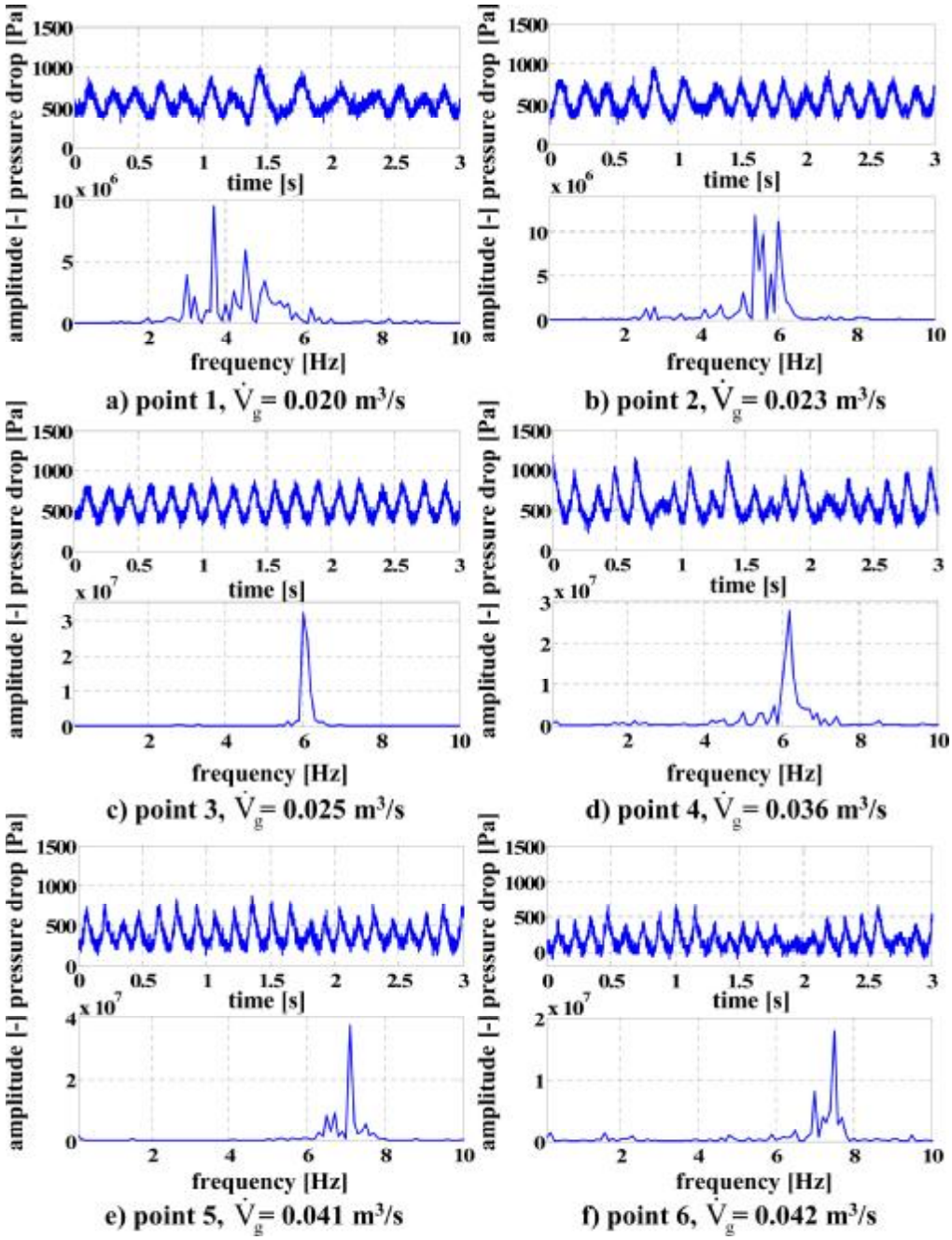

Figure 3 Measured bed pressure drop fluctuations (top) and Fourier-transformation of the frequency spectra of these fluctuations (bottom).

Re-G-Ar diagram by experimental data

The preceding analysis of the gas phase pressure fluctuations and the visual observations have illustrated how one can determine different hydrodynamic operation ranges of the investigated spouted bed apparatus. For each parameter set, one point for the beginning of stable spouting can be included into the Re-G-Ar diagram. Re is the Reynolds number at the inlet at the beginning of stable spouting and G is a geometric ratio between the gas inlet area and the apparatus cross section

area at the fixed bed height. The results of the investigated acryl-glass spouted bed apparatus with slit-shaped gas inlets are depicted in Figure 4. Here, curve i denotes the beginning and curve j the end of stable spouting.

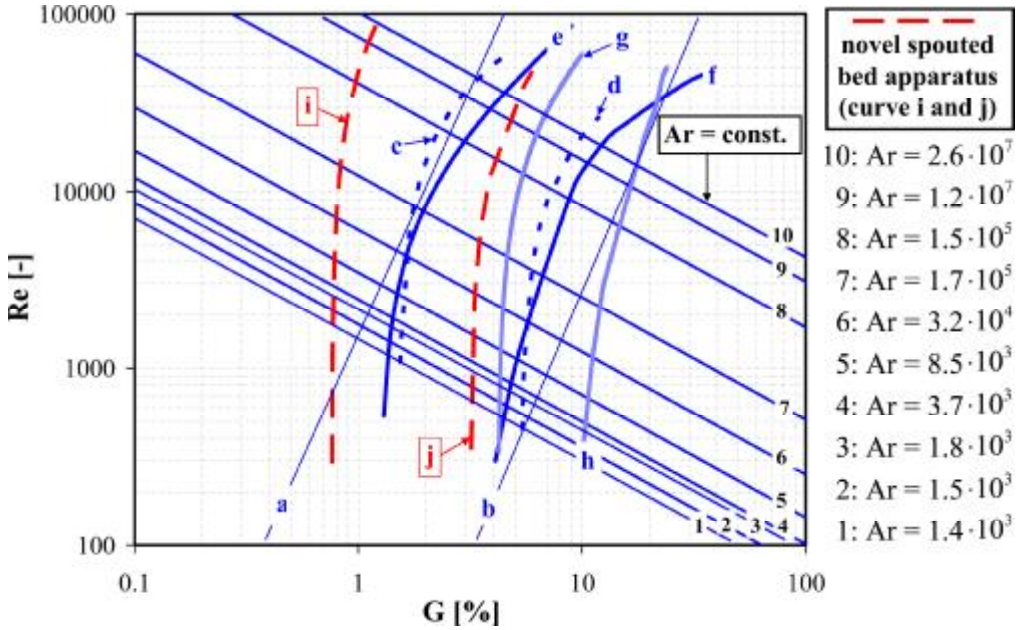

Figure 4 Re-G-Ar-Diagram.

The lines 1-10 are the lines of constant Archimedes number and the curves a-h are the boundaries of stable operation for different apparatuses. The region between the curves a and b is the range of stable operation of a conventional fluidized bed. For a prismatic spouted bed apparatus with two parallel gas inlets by Piskova [3], [4] this range is confined by the curves c and d. Furthermore, the stable operation range for a conical spouted bed apparatus is between the curves e and f (Olazar et al. [12]) and for a prismatic spouted bed apparatus with one gas inlet between the curves g and h (Mitev [13]). With the aid of this diagram comparisons between the different apparatus types can be made and the choice of an appropriate apparatus for a certain product is considerably facilitated.

2. CFD Continuum Modelling

In our continuum simulations we consider two phases: a gas phase (air) and a granular solid phase (γ-Al_2O_3-particles). In this model type all contributing phases are treated as continua that can fully interpenetrate. Due to the continuum description, supplementary closures for the particle-particle or particle-wall interactions are required. Thus, the kinetic theory of granular flow is incorporated in FLUENT 6.2 to account for the dependency of the rheological material properties on the local particle concentration and on the local particle fluctuating velocity due to particle collisions. In Table 1, the basic equations of the continuum model are presented.

Table 1: Equations of the continuum model.

Phasic volume fraction	$\sum_{q=1}^{n} \varepsilon_q = 1$	Eq (1)
Continuity equation for phase q	$\frac{\partial}{\partial t}\left(\varepsilon_q \rho_q\right) + \nabla \cdot \left(\varepsilon_q \rho_q \vec{v}_q\right) = 0$	Eq (2)
Momentum balance equation for phase q	$\frac{\partial}{\partial t}\left(\varepsilon_q \rho_q \bar{v}_q\right) + \nabla \cdot \left(\varepsilon_q \rho_q \vec{v}_q \vec{v}_q\right) = -\varepsilon_q \nabla p + \nabla \cdot \bar{\bar{\tau}}_q + \vec{R}_{pq}$	Eq (3)

Interphase force	$\sum_{p=1}^{n} \vec{R}_{pq} = \sum_{p=1}^{n} K_{pq}\left(\vec{v}_p - \vec{v}_q\right)$	Eq (4)

In the momentum balance equation $\bar{\bar{\tau}}_q$ denotes the stress tensor of phase q and is calculated as follows:

$$\bar{\bar{\tau}}_q = \varepsilon_q \mu_q \left(\nabla \vec{v}_q + \nabla \vec{v}_q^{\,T}\right) + \varepsilon_q \left(\lambda_q - \frac{2}{3}\mu_q\right) \nabla \cdot \vec{v}_q \bar{\bar{I}} \qquad \text{Eq (5)}$$

Here, μ_q (μ_s for the solid phase) is the shear viscosity of the solid phase as defined in the kinetic theory of granular flow. The solid shear stress tensor contains shear and bulk viscosities arising from particle momentum exchange due to translation ($\mu_{s,kin}$) and collision ($\mu_{s,col}$). Furthermore, a frictional component of viscosity ($\mu_{s,fr}$) is included to account for the viscous-plastic transition that occurs when particles of a solid phase reach the maximum solid volume fraction. All three contributions are considered additively:

$$\mu_s = \mu_{s,col} + \mu_{s,kin} + \mu_{s,fr} \qquad \text{Eq (6)}$$

The collisional part of the shear viscosity $\mu_{s,col}$ is modelled as following:

$$\mu_{s,col} = \frac{4}{5}\varepsilon_s \rho_s d_s g_{0,ss}\left(1 + e_{ss}\right)\left(\frac{\theta_s}{\pi}\right)^{1/2} \qquad \text{Eq (7)}$$

The kinetic part $\mu_{s,kin}$ is calculated by the expression of Gidaspow et al. [14]:

$$\mu_{s,kin} = \frac{10\rho_s d_s \sqrt{\theta_s \pi}}{96\varepsilon_s\left(1 + e_{ss}\right) g_{0,ss}}\left[1 + \frac{5}{4} g_{0,ss}\varepsilon_s\left(1 + e_{ss}\right)\right]^2 \qquad \text{Eq (8)}$$

The frictional contribution $\mu_{s,fr}$ is accounted for by the expression of Schaeffer [10]:

$$\mu_{s,fr} = \frac{p_s \sin\phi_i}{2\sqrt{I_{2D}}} \qquad \text{Eq (9)}$$

where ϕ_i is the angle of internal friction. This value accounts for loss of momentum due to the friction between the particles. In this work a study under variation of the angle of internal friction ϕ_i will be presented. Moreover, a simulation without consideration of frictional contributions will be shown to examine the significance of the incorporation of inter-particle friction in multiphase continuum simulations of spouted beds.

For description of the gas-particle interactions the Clift et al. [8] drag model is used. This model consists of ten different correlations for the drag coefficient C_D in dependency of the particle Reynolds number. The gas-particle moment exchange coefficient K_{gs} (see Eq (4)) is calculated as follows:

$$K_{gs} = \frac{\varepsilon_s \rho_s f}{\tau_s} \qquad \text{Eq (10)}$$

Where f is the drag function and is calculated by:

$$f = \frac{C_D\, Re}{24} \qquad \text{Eq (11)}$$

The following correlations for the drag coefficient C_D are used in this model:

$$
\begin{aligned}
&C_D = 3/16 + 24/\mathrm{Re} && \mathrm{Re} \le 0.01 \\
&C_D = 24/\mathrm{Re}\left[1 + 0.1315\,\mathrm{Re}^{0.82-0.05\,w}\right] && 0.01 < \mathrm{Re} \le 20 \\
&C_D = 24/\mathrm{Re}\left[1 + 0.1935\,\mathrm{Re}^{0.6305}\right] && 20 < \mathrm{Re} \le 260 \\
&\log_{10} C_D = 1.6435 - 1.242w + 0.1558w^2 && 260 < \mathrm{Re} \le 1{,}500 \\
&\log_{10} C_D = -2.4571 + 2.558w - 0.929w^2 + 0.1049w^3 && 1{,}500 < \mathrm{Re} \le 12{,}000 \\
&\log_{10} C_D = -1.9181 + 0.6370w + 0.063w^2 && 12{,}000 < \mathrm{Re} \le 44{,}000 \\
&\log_{10} C_D = -4.3390 + 1.5809w - 0.1546w^2 && 44{,}000 < \mathrm{Re} \le 338{,}000 \\
&C_D = 29.78 - 5.3w && 338{,}000 < \mathrm{Re} \le 400{,}000 \\
&C_D = -0.49 + 0.1w && 400{,}000 < \mathrm{Re} \le 1000{,}000 \\
&C_D = 0.19 - 8 \cdot 10^4/\mathrm{Re} && \mathrm{Re} > 1000{,}000 \\
&\text{where } w = \log_{10} \mathrm{Re}
\end{aligned}
\qquad \text{Eq (12)}
$$

For more detailed information on the applied continuum model we refer to Gryczka et al. [5], [6], [**7**]. The equations of the multiphase continuum model were solved by means of a finite volume technique provided in the commercial software FLUENT 6.2. An entire geometry model of the spouted bed apparatus was created and meshed. Mesh independence of the simulation results was obtained by variation of the number of mesh elements. The time step size was 10^{-4} seconds. Convergence of the solution was assumed at a residual value of 10^{-3}. The gas volume flow was set to a constant value of 0.041 m^3/s.

Simulation results

Following, the calculated distributions of the granular solid phase ε_s under variation of the angle of internal friction (ϕ_i=25, 30, 35, 40°) and without considering friction are compared with images taken during the experiment (see Figure 5). Furthermore, measured and calculated gas phase pressure fluctuations are compared in Figure 6 to do even more accurate comparisons between the simulations and the experiment.

The real fluidization process can be followed by the series of images in Figure 5a. Particles are sucked into the jet zone by the gas flow in the lower section of the process chamber and are subsequently accelerated vertically. Then, the particles are separated towards the apparatus walls in the fountain zone and afterwards they move back to the jet zone on the inclinations of the apparatus in the backflow zone. Thus, a circulating and uniform particle motion is obtained in this spouted bed apparatus. From Figure 5a it can also be recognized that the gas jet passes the bed material not straightforwardly, but is diverted to the left and to the right due to gas phase turbulence and non-ideal particle collisions. Also the formation of gas bubbles can be observed, which burst on the bed surface affecting gas phase pressure impulses. In Figure 6a, the gas phase pressure fluctuations of the experiment for an interval of 3 seconds are depicted, along with the measured pressure spectrum resulting from fast Fourier transformation (FFT). The recording frequency of the pressure values was 1 kHz both in the experiment and in the simulations. It is observable that fairly uniform pressure impulses with equal amplitudes are detected (Figure 6a top). This results in a large dominant peak in the FFT (Figure 6a bottom). The position of this peak on the x-axis reflects the frequency of the main fluctuation. In this case, the main frequency can be found around 6 - 7 Hz concluding that 6 - 7 gas bubbles burst on the bed surface regularly and with equal intensity during one second.

Figure 5b to 5e show images of the simulation of the distribution of the granular solid phase ε_s under variation of the angle of internal friction ϕ_i. A change of that value leads to a change of the solid shear stress tensor τ (Eq (5)) and thus has an effect on the moment balance equation (Eq (3)).

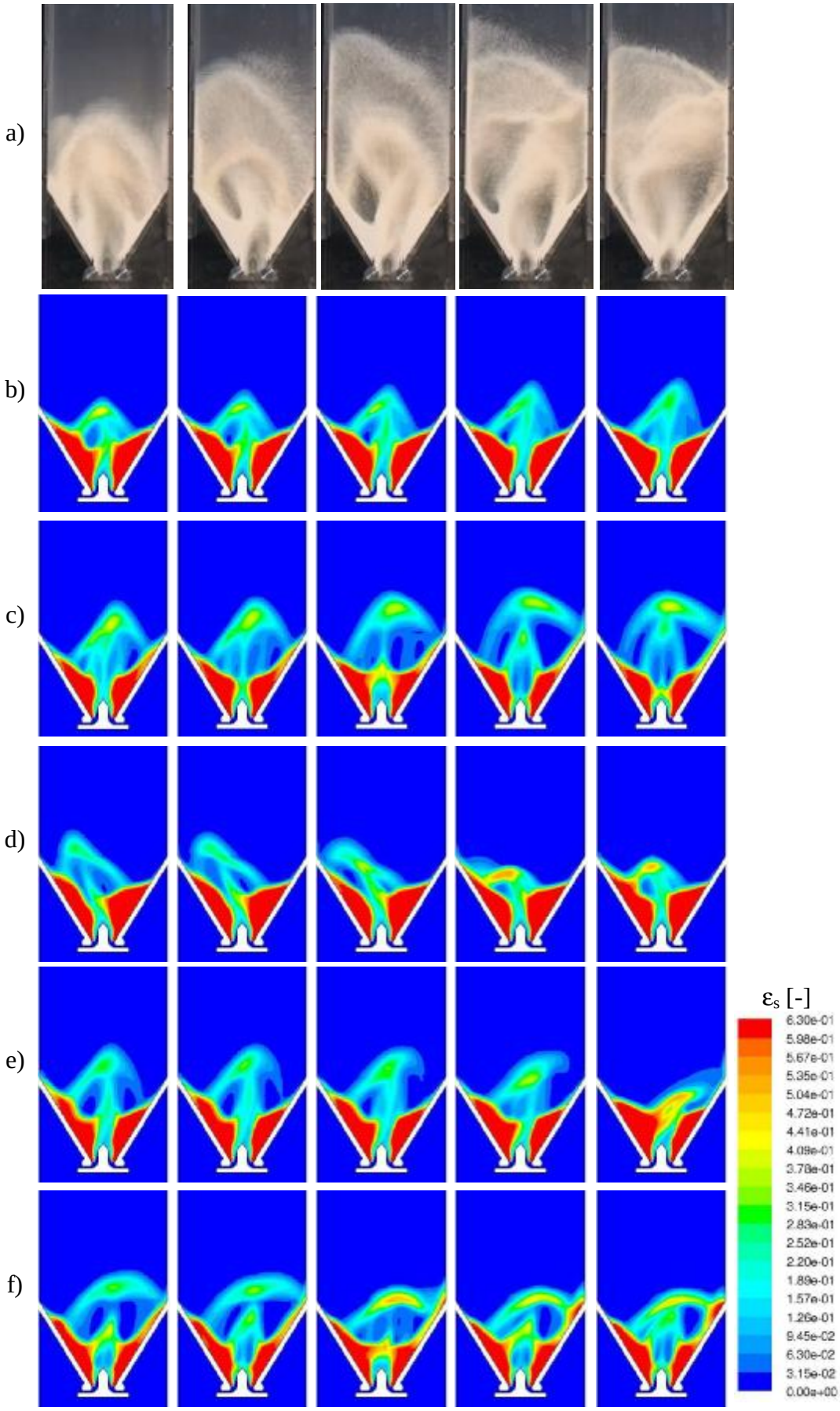

Figure 5 Volume fraction ε_s of the granular solids phase. Gas throughput 0.041 m^3/s, Clift et al. [8] drag model. a) Experiment, b) ϕ_i=25°, c) ϕ_i=30°, d) ϕ_i=35°, e) ϕ_i=40°, f) no friction. Time between images: 0.1 seconds.

Consequently, different hydrodynamics are calculated in dependency of the angle of internal friction (see Figure 5b to 5e). However, the calculated distributions of the granular solids phase ε_s do not show dramatically big differences. The hydrodynamic behaviour in this spouted bed is predominantly affected by the force exposure of the gas on the particles in the jet zone where the particle concentration is between 20 and 30 %. Here, the influence of the frictional contributions on the total bed behaviour is nearly negligible. In regions with a high solids concentration (backflow zones) where the particles are under sustained contact, the friction between the particles has to be accounted for to obtain realistic simulation results. The best fit with the experiment is given in Figure 6c with ϕ_i=30°. Here, the bed expansion is the highest in comparison to the simulations with ϕ_i =25°, ϕ_i =35° or ϕ_i =40° (Figure 5b, d and e). However, it is slightly under-predicted in comparison to the experiment (Figure 5a) as already reported by Gryczka et al. [6]. The angle of internal friction of ϕ_i =30° is according to Antonyuk et al. [9] a realistic value for the experimental material.

The series of images (Figure 5f) of the simulation without frictional contributions ($\mu_{s,fr}$ = 0 in Eq (6)) shows a surprisingly good resemblance with the experiment. The spout channel is wider

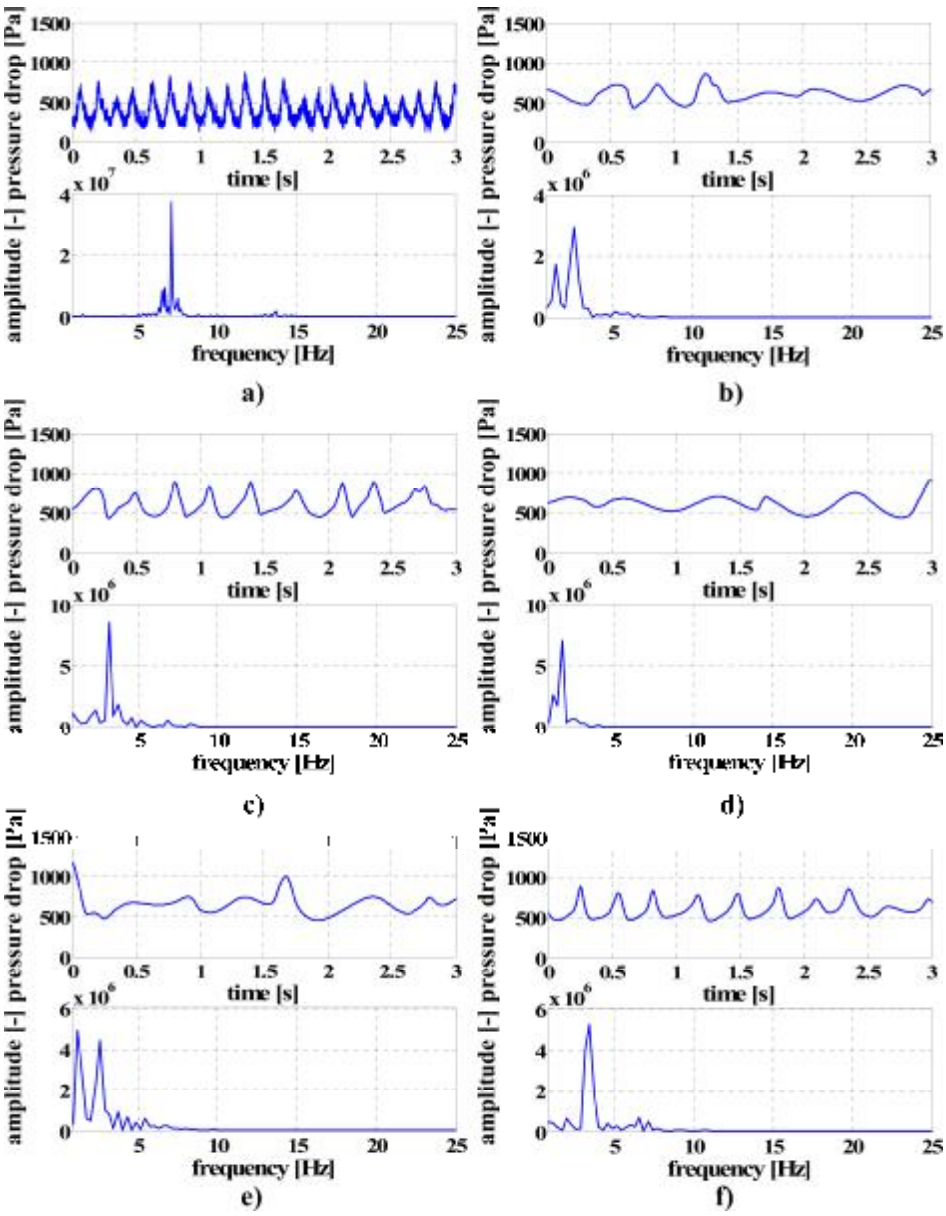

Figure 6 Bed pressure drop fluctuations (top) and Fourier transformation of the frequency spectra of the fluctuations (bottom). a) Experiment, b) ϕ_i=25°, c) ϕ_i =30°, d) ϕ_i =35°, e) ϕ_i =40°, f) no friction.

compared to all simulations with consideration of friction which is also in agreement with the experiment. Due to the neglect of the frictional contribution $\mu_{s,fr}$ in the momentum balance equation (Eq (6)), a more intensive interaction between the jet zone and the backflow zone is enabled. That means that because of the lower viscosity μ_s of the particle assembly, the force exposed by the fluidization gas has a higher impact on the motion of the particle assembly compared to the case with consideration of friction where the higher viscosity prevents the separation of the particles.
Comparing the simulated and measured gas phase pressure fluctuations and the Fourier analysis on these spectra (Figure 6) it also becomes clear that the best resemblance with the experiment is achieved with ϕ_i =30° when friction is accounted for. In accordance to the measurement the calculated pressure spectrum shows a periodic behaviour with fairly equal amplitudes concluding that equal sized gas bubbles rise through the bed and burst on the surface affecting the pressure fluctuations. However, due to the under-prediction of bed expansion the intensity of the simulated pressure impulses are somewhat lower compared to the experiment. That also results in the lower frequency of bursting gas bubbles in the Fourier analysis predicted by the continuum model (ca. 3 Hz, see Figure 6c) in comparison to the experiment (ca. 7 Hz, see Figure 6a). The same statements are valid for the simulation without consideration of friction (see Figure 6f). The gas phase pressure fluctuations are also periodic and exhibit equal amplitudes which results in clear peak in the Fourier analysis.
In summary, it can be stated that there is an influence of the friction between the particles on the spouted bed hydrodynamic behaviour, however, which is not very big. Other effects (gas-particle interactions or particle collisions) have a higher impact on the total bed behaviour. The best fit with the experiment was obtained with an angle of internal friction of ϕ_i =30° in Schaeffer`s [10] model which was found to be a realistic value for the experimental material (Antonyuk et al. [9]). The simulation without consideration of friction has also demonstrated that the influence of friction by application of Schaeffer`s [10] model in this spouted bed apparatus is not very big. However, from literature it is known that Schaeffer`s [10] empirical frictional viscosity model which is based on soil mechanical principles is not the first choice to simulate the spouted bed hydrodynamics. More detailed models (Laux [15], Ocone et al. [16], Syamlal et al. [17]) which describe the frictional contributions in a more physical based manner should be incorporated in the continuum model to eventually come to any conclusions. Moreover, the application of the new fluid mechanic approach which allows for a smooth transition from different flow regimes (dilute, intermediate-dense, dense) to another using a unified model (Tardos [18], Savage [19]) should also be taken into account in the continuum simulations in future (Makkawi and Ocone [20]).

3. Industrial Applications of the Novel Spouted Bed

For industrial purpose the novel spouted bed principle has been further developed to apply this for spray granulation, coating, agglomeration and thermal treatment of particulate solids. Some recent developments about this technology are explained in [21], [22], [23] and [24].
The Glatt company improved the patented ProCell-apparatus by integrating different types of spray systems into a single or multi-stage process chamber as described in Figure 7.
Due to the specific fluidization behaviour and the related principle of particle movement inside the process chamber, the ProCell has process advantages compared to conventional fluidized beds:

- fluidization of large particles and irregular formed particles
- fluidization of fine particles
- fluidization of products with wide particle size distribution
- gently drying of temperature-sensitive products
- stability of processing due to the reduced risk of blockages of the gas distributor
- possible reduction of residence time in process chamber

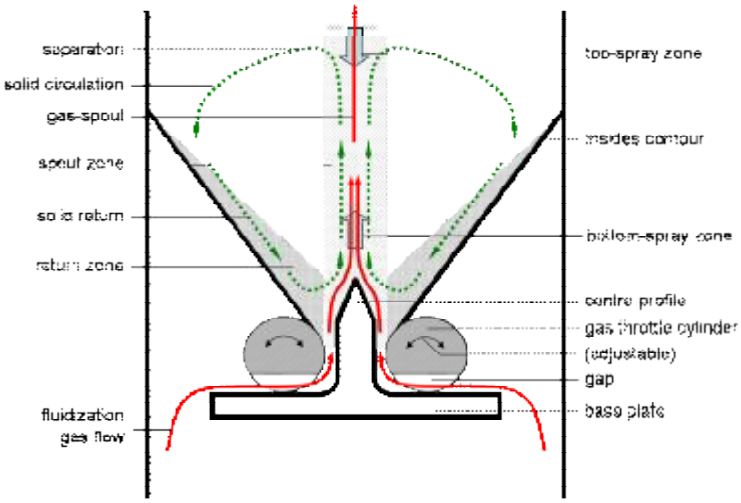

Figure 7 Principle of a Glatt- ProCell-apparatus (courtesy of Glatt/Germany).

As a typical field of application we want to refer to the spray granulation. In spray granulation processes a liquid containing a dissolved, suspended or molten solid is dried or solidified in such a way that compact and dense granules are produced in one process step. The basic principle is schematically shown in Figure 8.

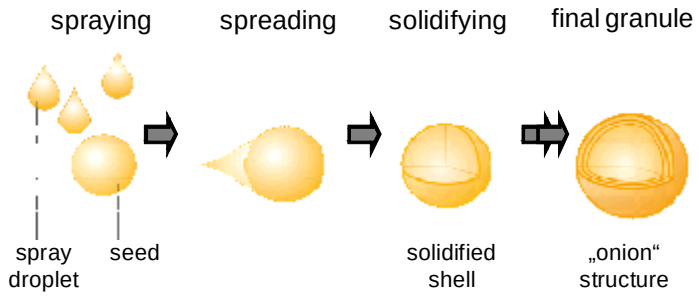

Figure 8 Principle of direct spray granulation (courtesy of Glatt/Germany).

As summarized above the ProCell has advantages compared to conventional fluidized beds when products are sensitive to thermal stress. For instance enzymes (e.g. for use in laundry or feed products) or encapsulated volatile substances (e.g. orange oil, PUFA) can be processed to create innovative product forms. In Figure 9 and 10 two typical products are shown.

Figure 9 Product sample: spray granulated enzyme formulation (courtesy of Glatt/Germany).

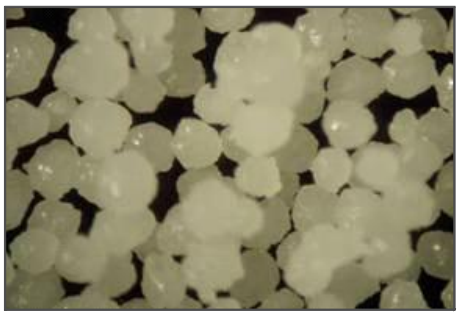

Figure 10 Product sample: spray granulated aroma oil emulsion (courtesy of Glatt/Germany).

The ProCell-apparatus is a commercial version of the novel spouted bed and available in different scales. Starting with the ProCell-LabSystem processes and products can be developed and optimized at laboratory scale (e.g. at 0.2 to 2 kg batch size or up to 2 kg/h in continuous operation). Additionally pilot scale industrial production units can be delivered in different executions (Figure 11).

Figure 11 Industrial scale granulation plant Glatt - ProCell 125 in closed loop operation (courtesy of Glatt/Germany).

4. Conclusions

In this work the fluidization behaviour of a novel spouted bed apparatus with two adjustable gas inlets was investigated. Different hydrodynamic operation ranges were identified by evaluation of gas phase pressure fluctuations and a subsequent Fourier analysis on these spectra. The stable operation domain was depicted in a Re-G-Ar diagram and comparisons between other fluidized and spouted beds were made.

Furthermore, the hydrodynamic behaviour was modelled by means of continuum approach in the commercial software package FLUENT 6.2. In this work, the influence of the friction between the particles on the hydrodynamic bed behaviour was studied by variation of the angle of internal friction ϕ_i in Schaeffer`s [10] model. Moreover, a simulation without consideration of frictional contributions was conducted. It was revealed that there are no big differences in the hydrodynamic behaviour in the tested range of values of angles of internal friction. However, the best resemblance with the experiment was achieved with a value of ϕ_i =30° that was proved to be a realistic value for the experimental material (Antonyuk et al. [9]). The neglect of frictional contributions also gave qualitative good results in comparison to the experiment. It seems that the influence of friction

described by Schaeffer`s [10] model is not very big. This simple frictional viscosity model is an empirical model based on soil mechanical principles and thus seems to be unable to capture the real complex frictional processes taking place during the spouted bed fluidization. Gryczka et al. [5], [6], [**7**] recently found out that the variation of the gas-particle drag model or the coefficient of restitution had a bigger influence on the simulated spouted bed hydrodynamic behaviour.
The transfer of the novel spouted bed to an industrial apparatus at different size scale was successful. Based on experimental and theoretical studies of the fluidization behaviour the scaling up can be carried out supported by CFD-simulations. Due to the innovative design of the Glatt ProCell-apparatus the particle motion and the fluid dynamics inside the process chamber can be directly influenced depending on the process requirements.

5. Acknowledgements

The DFG is gratefully acknowledged for funding this project within the Research Training Group 828 “Micro-Macro Interactions of structured media and particle systems”.

6. Nomenclature

Ar	Archimedes number	[-]
C_D	drag coefficient	[-]
d_s	particle diameter	[m]
e	coefficient of restitution	[-]
f	drag function	[-]
g	acceleration of gravity	[m/s^2]
G	geometric ratio	[-]
$g_{0,ss}$	radial distribution function	[-]
K_{gs}	gas-solid exchange coefficient	[-]
p	pressure	[Pa]
$\vec{R}$	interaction force	[N]
Re	Reynolds number	[-]
$\vec{v}$	velocity	[m/s]
$\dot{V}_g$	gas volume flow	[m^3/s]

Greek letters

ε	volume fraction	[-]
Θ	sphericity	[-]
θ	granular temperature	[m^2/s^2]
λ	granular bulk viscosity	[kg/(m s)]
μ	dynamic viscosity	[Pa s]
ν	kinematic viscosity	[m^2/s]
ρ_s	solids density	[kg/m^3]
τ	stress tensor	[-]
τ_s	particulate relaxation time	[s]
ϕ_i	angle of internal friction	[°]

Subscripts

col-collision

fr	friction
g	gas
gs	gas-solid
in	inlet
kin	kinetic
p, q	phase indication
s	solid
ss	solid-solid

7. References

1. Mitev. D.T., 1979. Theoretische und experimentelle Untersuchung der Hydrodynamik, des Wärme- und Stoffüberganges in Strahlschichtapparaten. (russ.), Habilitation, LTI Leningrad.

2. Kojouharov K., 2004. Entwicklung einer neuen Anströmeinrichtung für Strahlschichten. Dissertation, Otto-von-Guericke-Universität Magdeburg.

3. Piskova, E., 2002. Untersuchung der Fluiddynamik eines Strahlschichtapparates mit zwei parallelen Gaseintritten und seine Anwendung auf die Beschichtung feindisperser Feststoffteilchen. Dissertation, Otto-von-Guericke-Universität Magdeburg.

4. Piskova, E., Kojouharov, K., Mitev, D., Krüger, G., Mörl, L., 2003. Spouted bed – con-structions of apparatuses, fluid dynamics and application. Journal of the University of Chemical Technology and Metallurgy, Sofia, Bulgaria, 38, 565-570.

5. Gryczka, O., Heinrich, S., Deen, N.G., van Sint Annaland, M., Kuipers, J.A.M., Jacob, M., Mörl, L., Characterization and CFD-modeling of the hydrodynamics of a prismatic spouted bed apparatus. In: Chem. Eng. Sc., in press, DOI: CES-S-08-00994.

6. Gryczka, O., Heinrich, S., Deen, N.G., Kuipers, J.A.M., Mörl, L.: CFD modeling of a prismatic spouted bed with two adjustable gas inlets. In: Can. J. Chem. Eng., in press.

7. Gryczka, O., Heinrich, S., Deen, N.G., Kuipers, J.A.M., Mörl, L., 2009. Three-Dimensional computational fluid dynamics modeling of a prismatic spouted bed. In: Chem. Eng. Technol. 32(3), 470-481.

8. Clift, R., Grace, J. R. Weber, M. E. 1978. Bubbles, Drops and Particles. Academic Press, New York.

9. Antonyuk, S., Heinrich, S. Tomas, J. Deen, N. G. van Buijtenen M. S. and Kuipers, J. A. M. 2008. Comparison of energy dissipation during the compression and impact of spherical elastic-plastic granules. In: Chem. Eng. Sc. (submitted)

10. Schaeffer, R.W. 1987. Instability in the evolution equations describing incompressible granular flow. In: J. Diff. Equ. 66, 19-50.

11. Huilin, L., Yurong, H., Wentie, L., Ding, J., Gidaspow, D., Bouillard, J. 2004. Computer simulations of gas–solid flow in spouted beds using kinetic–frictional stress model of granular flow. In: Chem. Eng. Sc. 59, 865-878.

12. Olazar, M.; San Jose, M. J.; Aguayo, A. T.; Arandes, J. M.; Bilbao, J., 1993. Design Factors of Conical Spouted Beds and Jet Spouted Beds. In: Ind. Eng. Chem. Res., 32, 1245-1250.

13. Mitev, D. T., 1967. Untersuchung der Wirbelschichthydrodynamik im prismatischen Apparat. (russ.) Dissertation, LTI Leningrad.

14. Gidaspow, D., Bezburuah, R., Ding, J., 1992. Hydrodynamics of circulating fluidized beds, kinetic theory approach. In Fluidization 7, Proceedings of the 7th Engineering Foundation Conference on Fluidization, 75-82.

15. Laux, H., 1998. Modelling of dilute and dense dispersed fluid-particle flow. Ph.D Thesis, NTNU Trondheim, Trondheim, Norway.

16. Ocone, R., Sundaresan, S., Jackson, R., 1993. Gas-particle flow in a duct of arbitrary inclination with particle-particle interaction. Fluid Mechanics and Transport Phenomena 39, 1261-1271.

17. Syamlal, M., Rogers, W.A., O'Brien, T.J., 1993. MFIX documentation and theory guide, DOE/METC94/ 1004, NTIS/DE94000087.

18. Tardos, G.I, McNamara, S., Talu, I., 2003. Slow and intermediate flow of frictional bulk powder in the coquette geometry. Powder Technology 131, 23-39.

19. Savage, S.B., 1983. In Jenike, J.T., Satake (Eds.). Proceedings of the US-Japan seminar on new models and constitutive relations in the mechanics of granular materials. Elsevier, Amsterdam, P. 261.

20. Makkawi, Y. Ocone, R., 2005. Modelling of particle stress at the dilute-intermediate-dense flow regimes: A review. KONA - Powder Science and Technology No.23, 49-63.

21. Glatt: Innovative Technologies for Granules and Pellets.- Glatt Ingenieurtechnik GmbH, Weimar/Germany, 2006 (company brochure).

22. Uhlemann, H.; Mörl, L., 2000. Wirbelschicht-Sprühgranulation, Springer, Berlin.

23. Jacob, M., 2007. Granulation Equipment. In: Salman,A.D.; Hounslow,M.J.; Seville, J.P.K. (Eds.): Handbook of powder Technology, Vol. 11, Granulation. Elsevier, Amsterdam.

24. Jacob, M.: ProCell technology: Modelling and Application. Powder Technology 189, 332-342.